

# Morphology and molecular phylogeny of three new deep-sea species of *Chrysogorgia* (Cnidaria, Octocorallia) from seamounts in the tropical Western Pacific Ocean

Yu Xu<sup>1,2,3,4</sup>, Zifeng Zhan<sup>1,2,3</sup>, Kuidong Xu<sup>Corresp. 1,2,3,4</sup>

<sup>1</sup> Laboratory of Marine Organism Taxonomy and Phylogeny, Institute of Oceanology, Chinese Academy of Sciences, Qingdao, China

<sup>2</sup> Laboratory for Marine Biology and Biotechnology, Pilot National Laboratory for Marine Science and Technology (Qingdao), Qingdao, China

<sup>3</sup> Center for Ocean Mega-Science, Chinese Academy of Sciences, Qingdao, China

<sup>4</sup> University of Chinese Academy of Sciences, Beijing, China

Corresponding Author: Kuidong Xu  
Email address: kxu@qdio.ac.cn

Three new species of *Chrysogorgia* were discovered from seamounts in the tropical Western Pacific Ocean. *Chrysogorgia dendritica* sp. nov. and *Chrysogorgia fragilis* sp. nov. were collected from the Kocebu Guyot of the Magellan Seamount chain with the water depth of 1,821 m and 1,279–1,321 m, respectively, and *Chrysogorgia gracilis* sp. nov. was collected from a seamount adjacent to the Mariana Trench with the water depth of 298 m. They all belong to the *Chrysogorgia* “group A, Spiculosae” with rods distributed in body wall and tentacles, and differ from all congeners except *C. abludo* Pante & Watling, 2012 by having a tree-shaped colony (vs. bottlebrush-shaped, planar or biflabellate). *Chrysogorgia dendritica* sp. nov. is unique in having a monopodial stem, the 1/3L branching sequence and the amoeba-shaped sclerites (sclerites branched toward to many directions) at the body bases of polyps. *Chrysogorgia fragilis* sp. nov. is most similar to *C. abludo*, but differs by the regular 1/3L branching sequence and elongate flat scales in coenenchyme. *Chrysogorgia gracilis* sp. nov. is easily separated from congeners by the 1/4L branching sequence, the absence of sclerites in the basal body wall, and the very sparse scales in coenenchyme. Based on the phylogenetic and genetic distance analyses of mtMutS gene, all the available *Chrysogorgia* species were separated into two main groups: one includes *C. binata*, *C. cf. stellata* and *C. chryseis*, which have two or more fans emerging from a short main stem (bi- or multi-flabellate colony); the other one includes all the species with the branching patterns as a single ascending spiral (clockwise or counterclockwise, bottlebrush-shaped colony), a fan (planar colony) and a bush of branches perched on top of a long straight stem (tree-shaped colony). Additionally, the tree-shaped colony represents a new branching pattern in *Chrysogorgia*, and therefore we extend the generic diagnosis.

1 **Morphology and molecular phylogeny of three new deep-sea species of *Chrysogorgia***  
2 **(Cnidaria, Octocorallia) from seamounts in the tropical Western Pacific Ocean**

3

4 Yu Xu<sup>1,2,3,4</sup>, Zifeng Zhan<sup>1,2,3</sup>, Kuidong Xu<sup>1,2,3,4</sup>

5

6 <sup>1</sup> Laboratory of Marine Organism Taxonomy and Phylogeny, Institute of Oceanology, Chinese  
7 Academy of Sciences, Qingdao, Shandong, China

8 <sup>2</sup> Laboratory for Marine Biology and Biotechnology, Pilot National Laboratory for Marine  
9 Science and Technology (Qingdao), Qingdao, Shandong, China

10 <sup>3</sup> Center for Ocean Mega-Science, Chinese Academy of Sciences, Qingdao, Shandong, China

11 <sup>4</sup> University of Chinese Academy of Sciences, Beijing, China

12

13 Corresponding Author: Kuidong Xu

14 7 Nanhai Rd., Qingdao, Shandong, 266071, China

15 Email address: kxu@qdio.ac.cn

16

17 **Abstract**

18 Three new species of *Chrysogorgia* were discovered from seamounts in the tropical Western  
19 Pacific Ocean. *Chrysogorgia dendritica* sp. nov. and *Chrysogorgia fragilis* sp. nov. were  
20 collected from the Kocebu Guyot of the Magellan Seamount chain with the water depth of 1,821  
21 m and 1,279–1,321 m, respectively, and *Chrysogorgia gracilis* sp. nov. was collected from a  
22 seamount adjacent to the Mariana Trench with the water depth of 298 m. They all belong to the  
23 *Chrysogorgia* “group A, Spiculosae” with rods distributed in body wall and tentacles, and differ  
24 from all congeners except *C. abludo* Pante & Watling, 2012 by having a tree-shaped colony (vs.  
25 bottlebrush-shaped, planar or biflabellate). *Chrysogorgia dendritica* sp. nov. is unique in having  
26 a monopodial stem, the 1/3L branching sequence and the amoeba-shaped sclerites (sclerites  
27 branched toward to many directions) at the body bases of polyps. *Chrysogorgia fragilis* sp. nov.  
28 is most similar to *C. abludo*, but differs by the regular 1/3L branching sequence and elongate flat  
29 scales in coenenchyme. *Chrysogorgia gracilis* sp. nov. is easily separated from congeners by the  
30 1/4L branching sequence, the absence of sclerites in the basal body wall, and the very sparse  
31 scales in coenenchyme. Based on the phylogenetic and genetic distance analyses of mtMutS gene,  
32 all the available *Chrysogorgia* species were separated into two main groups: one includes *C.*  
33 *binata*, *C. cf. stellata* and *C. chryseis*, which have two or more fans emerging from a short main  
34 stem (bi- or multi-flabellate colony); the other one includes all the species with the branching  
35 patterns as a single ascending spiral (clockwise or counterclockwise, bottlebrush-shaped colony),  
36 a fan (planar colony) and a bush of branches perched on top of a long straight stem (tree-shaped  
37 colony). Additionally, the tree-shaped colony represents a new branching pattern in  
38 *Chrysogorgia*, and therefore we extend the generic diagnosis.

39

40 **Keywords** Anthozoa, Chrysogorgiidae, *Chrysogorgia dendritica*, *Chrysogorgia fragilis*,

41 *Chrysogorgia gracilis*, taxonomy

42

### 43 **Introduction**

44 The genus *Chrysogorgia* Duchassaing & Michelotti, 1864 contains 72 species distributed in the  
45 world oceans, with water depths ranging from 10 m to 4492 m ([Watling et al., 2011](#); [Pante et al.,](#)  
46 [2012](#); [Cairns, 2018](#); [Xu et al., 2019](#)). Three branching forms have been recognized in the  
47 colonies of the genus: a single ascending spiral (clockwise or counterclockwise) producing a  
48 bottlebrush shape, a single fan (planar colony) and two fans emerging from a short main stem  
49 (biflabellate colony) ([Pante & Watling, 2012](#); [Cordeiro et al., 2015](#)). Based on the shapes of rods  
50 or scales in the body wall and tentacles, a rough grouping has been built for the separation of  
51 *Chrysogorgia* species. Versluys ([1902](#)) divided the genus *Chrysogorgia* into three groups, which  
52 were summarized by Cairns ([2001](#)) as “group A, Spiculosae”, “group B, Squamosae aberrantes”,  
53 and “group C, Squamosae typicae”. Cordeiro et al. ([2015](#)) supplemented the fourth group “group  
54 D, Spiculosae aberrantes”, which contains only the species *C. upsilonia* Cordeiro, Castro &  
55 Pérez, 2015.

56 While studying the benthic diversity in the tropical Western Pacific Ocean, we collected  
57 four specimens of *Chrysogorgia*. Based on morphological and phylogenetic analyses, we  
58 describe these specimens as three new species: *C. dendritica* sp. nov., *C. fragilis* sp. nov. and *C.*  
59 *gracilis* sp. nov. Their genetic distances and single mutations on mtMutS as well as phylogenetic  
60 relationships within *Chrysogorgia* species are discussed.

61

### 62 **Materials & Methods**

63

#### 64 **Specimen collection and morphological examination**

65 Specimens were obtained by the remotely operated vehicle (ROV) *FaXian* (Discovery) from an  
66 unnamed seamount (temporarily named as M2) adjacent to the Mariana Trench and the Kocebu  
67 Guyot in the Magellan Seamounts in the tropical Western Pacific Ocean during the cruises of the  
68 R/V *KeXue* (Science) in 2016 and 2018 (Fig. 1). These specimens were photographed *in situ*  
69 before sampled, photographed on board and then stored in 75% ethanol after collection. Some  
70 branches were detached and stored at -80°C for molecular analysis.

71 The general morphology and anatomy were examined by using a stereo dissecting  
72 microscope. The sclerites of the polyps and branches were isolated by digestion of the tissues in  
73 sodium hypochlorite, and then were washed with deionized water repeatedly. Polyps and  
74 sclerites were air-dried and mounted on carbon double adhesive tape and coated for the Scanning  
75 Electron Microscope (SEM) to investigate their structure. SEM scans were obtained and the  
76 optimum magnification was chosen for each kind of sclerites by using TM3030Plus SEM.

77 The morphological terminology follows Bayer et al. ([1983](#)), with which we coin the  
78 following new terms to describe the shape of sclerites. Tree-shaped colony: a bush of branches  
79 perched on top of a long straight stem, forming a tree shape. Example: *Chrysogorgia dendritica*  
80 sp. nov. (Fig. 2A). Amoeba-shaped sclerite: sclerites branched toward to many directions, varied  
81 in shape like an amoeba. Example: *Chrysogorgia dendritica* sp. nov. (Fig. 3C).

82 The type specimens of the three new species have been deposited in the Marine Biological  
83 Museum of Chinese Academy of Sciences (MBMCAS) at Qingdao, China.

84

#### 85 **DNA extraction and sequencing**

86 Total genomic DNA was extracted from the polyps of each specimen using the TIANamp  
87 Marine Animal DNA Kit (Tiangen Bio. Co., Beijing, China) following the manufacturer's  
88 instructions. PCR amplification for the mitochondrial genomic region 5'-end of the DNA  
89 mismatch repair protein – *mutS* – homolog (mtMutS) was conducted using primers  
90 AnthoCorMSH (5'-AGGAGAATTATTCTAAGTATGG-3'; [Herrera et al., 2010](#)) and Mut-  
91 3458R (5'-TSGAGCAAAAGCCACTCC-3'; [Sánchez et al., 2003](#)). PCR reactions were  
92 performed using I-5™ 2 × High-Fidelity Master Mix DNA polymerase (TsingKe Biotech,  
93 Beijing, China). The amplification cycle conditions were as follow: denaturation at 98°C for 2  
94 min, followed by 32 cycles of denaturation at 98°C for 20 s, annealing at 50°C for 20 s,  
95 extension at 72°C for 15 s, and a final extension step at 72°C for 2 min. PCR purification and  
96 sequencing were performed by TsingKe Biological Technology (TsingKe Biotech, Beijing,  
97 China).

98

#### 99 **Genetic distance and phylogenetic analyses**

100 The mtMutS may be the most variable mitochondrial gene in octocorals ([Herrera et al., 2010](#);  
101 [McFadden et al., 2011](#); [Li et al., 2017](#)), and we selected this marker for molecular identification  
102 and phylogenetic analyses. All the available mtMutS sequences of *Chrysogorgia* spp. and the  
103 out-group species from related chrysogorgiid genera were downloaded from GenBank. The  
104 sequences from duplicate isolates or without associated publications or named *Chrysogorgia* sp.  
105 or containing sequencing errors (marked with “n” or “y” in the original sequences) were omitted  
106 from the molecular analyses. To correct possible mistakes, all the selected sequences were  
107 visually inspected, and translated to amino acids (AA) to insure all the AA sequences not  
108 including stop codons and suspicious substitutions. The nucleotide and AA sequences were  
109 aligned using MAFFT v.7 ([Katoh & Standley, 2013](#)) with the G-INS-i algorithm. With the  
110 guidance of the AA alignment, the nucleotide alignment was refined using BioEdit v7.0.5 (Hall,  
111 1999), and only the nucleotide alignment was used in the subsequent analyses. Genetic distances,  
112 calculated as uncorrected “*p*” distances within each species and among species, were estimated  
113 using MEGA 6.0 ([Tamura et al., 2013](#)).

114 For the phylogenetic analyses, only one sequence was randomly selected from the  
115 conspecific sequences without genetic divergence. The evolutionary model GTR+G was the  
116 best-fitted model for mtMutS, selected by AIC as implemented in jModeltest2 ([Darriba et al.,](#)  
117 [2012](#)). Maximum likelihood (ML) analysis was carried out using PhyML-3.1 ([Guindon et al.,](#)  
118 [2010](#)). For the ML bootstraps, we consider values < 70% as low, 70–94% as moderate and ≥ 95%  
119 as high following Hillis & Bull ([1993](#)). Node support came from a majority-rule consensus tree  
120 of 1 000 bootstrap replicates. Bayesian inference (BI) analysis was carried out using MrBayes  
121 v3.2.3 ([Ronquist & Huelsenbeck, 2003](#)) on CIPRES Science Gateway. Posterior probability was

122 estimated using four chains running 10 000 000 generations sampling every 1 000 generations.  
123 The first 25% of sampled trees were considered burn-in trees. Convergence was assessed by  
124 checking the standard deviation of partition frequencies ( $< 0.01$ ), the potential scale reduction  
125 factor (ca. 1.00), and the plots of log likelihood values (no obvious trend was observed over  
126 time). For the Bayesian posterior probabilities, we consider values  $< 0.95$  as low and  $\geq 0.95$  as  
127 high following Alfaro et al. (2003). The GenBank accession numbers of the mtMutS sequences  
128 were listed next to the species names in the phylogenetic tree.

129

### 130 **ZooBank registration**

131 The electronic version of this article in Portable Document Format (PDF) will represent a  
132 published work according to the International Commission on Zoological Nomenclature (ICZN),  
133 hence the new names contained in the electronic version are effectively published under that  
134 Code from the electronic edition alone. This published work and the nomenclatural acts it  
135 contains have been registered in ZooBank, the online registration system for the ICZN. The  
136 ZooBank Life Science Identifiers (LSIDs) can be resolved and the associated information viewed  
137 through any standard web browser by appending the LSID to the prefix <http://zoobank.org/>. The  
138 LSID for this publication is: urn:lsid:zoobank.org:pub:00D5E053-EFF8-4142-8D16-  
139 AAFC17D028E2. The online version of this work is archived and available from the following  
140 digital repositories: PeerJ, PubMed Central, and CLOCKSS.

141

### 142 **Results**

143

#### 144 **Class Anthozoa Ehrenberg, 1834**

#### 145 **Subclass Octocorallia Haeckel, 1866**

#### 146 **Order Alcyonacea Lamouroux, 1812**

#### 147 **Suborder Calcaxonia Grasshoff, 1999**

#### 148 **Family Chrysogorgiidae Verrill, 1883**

#### 149 **Genus *Chrysogorgia* Duchassaing & Michelotti, 1864**

150

#### 151 ***Chrysogorgia dendritica* sp. nov. (Figs. 2 and 3; Table 1)**

152 urn:lsid:zoobank.org:act:F0050AD3-9E65-4B03-8D26-2C687018DCAD

153

154 **Holotype.** MBM286354, station FX-Dive 178 (17°20.18'N, 152°41.85'E), Kocebu Guyot, depth  
155 1,821 m, 12 April 2018. GenBank accession number: MN510469.

156 **Diagnosis.** *Chrysogorgia* “group A, Spiculosae” with a long monopodial stem and a branching  
157 part on the top. Branching sequence 1/3L. Branches nearly perpendicular to stem, subdivided  
158 dichotomously. Polyps with a long neck and an expanded base. Rods and spindles in tentacles  
159 and polyp neck coarse with many warts. Scales and rare plates at polyp body base flat and  
160 amoeba-shaped. Scales in coenenchyme thin with irregular edges.

161 **Description.** Specimen about 57 cm long with the holdfast not recovered. Colony tree-shaped,  
162 composed of a 36 cm long, straight and unbranched stem and a 21 cm long branched part with

163 branching sequence 1/3L. The whole stem monopodial from bottom to top with lateral branches  
164 producing on the top. Stem surface almost smooth with a strong golden metallic luster, about 2  
165 mm in diameter at base (Figs. 2A, 2B). Branches subdivided dichotomously, up to seventh order,  
166 most broken after collection. Distance between adjacent branches 16–22 mm, and orthostiche  
167 interval 50–55 mm. First branch internodes 15–20 mm long, with the terminal branchlets up to  
168 50 mm. Polyps with a long neck and an expanded base, about 3 mm long and 2 mm wide at  
169 bases, composed of one or two on the first internodes, one to five in middle internodes, and up to  
170 six in terminal branchlets (Figs. 2C, 2D). No polyps on main axis internodes. Golden eggs often  
171 occurred at the expanded bases.

172 Rods longitudinally arranged in the back of tentacles, occasionally branched, with many  
173 small warts on surface, measuring  $77\text{--}330 \times 15\text{--}34 \mu\text{m}$  (Figs. 2E, 3H–3M). Sclerites rarely  
174 extend into the pinnules, which are otherwise sclerite-free. Spindles and rods longitudinally  
175 arranged in the long polyp neck, slender with many small warts on surface, usually slightly  
176 curved, measuring  $193\text{--}800 \times 25\text{--}56 \mu\text{m}$  (Figs. 3A–3G). Scales and rare plates transversely and  
177 crosswise arranged at body base, flat and amoeba-shaped with irregular edges, measuring  $69\text{--}$   
178  $248 \times 11\text{--}79 \mu\text{m}$  (Figs. 3N–3X). Scales of coenenchyme sparse, flat and lobed with irregular  
179 edges, measuring  $68\text{--}268 \times 10\text{--}70 \mu\text{m}$  (Figs. 3Y–3GG).

180 **Type locality.** Kocebu Guyot in the Magellan Seamount chain with water depth of 1,821 m.

181 **Etymology.** The Latin adjective *dendriticus* (dendritic) refers to the dendritic shape of the colony.

182 **Distribution and Habitat.** Found only on the Kocebu Guyot, where the colony attached to a  
183 died sponge (Fig. 2A). The water temperature was about  $2.31^\circ\text{C}$  and the salinity about 35.8 psu.

184 **Remarks.** *Chrysogorgia dendritica* sp. nov. has a monopodial stem (Fig. 2B), which makes it  
185 appear to be a member of the chrysogorgiid genus *Metallogorgia* Versluys, 1902. However, the  
186 new species is characterized by a series of features matching the genus *Chrysogorgia*  
187 Duchassaing & Michelotti, 1864. These include the flexible branches, dichotomously subdivided  
188 branches not forming a sympodia, relatively large polyp with an expanded base and a narrow  
189 neck, and well differentiated coenenchyme usually with more sclerites. The new species also  
190 resembles to the genus *Pseudochrysogorgia* Pante & France, 2010 in the monopodial stem, but  
191 differs by the obviously different polyps and the absence of ornamented sclerites. Our  
192 phylogenetic analysis (see below) supports this assignment as well. *Chrysogorgia dendritica* sp.  
193 nov. is distinctly different from congeners by its unique monopodial stem and the amoeba-  
194 shaped sclerites at the body bases.

195

196 *Chrysogorgia fragilis* sp. nov. (Figs. 4 and 5; Table 1)

197 urn:lsid:zoobank.org:act:562CFDA7-88F5-4D81-8FE5-BDE1F56A3EEC

198

199 **Holotype.** MBM286351, station FX-Dive 172 ( $17^\circ 23.64'\text{N}$ ,  $153^\circ 6.07'\text{E}$ ), Kocebu Guyot, depth  
200 1,321 m, 1 April 2018. GenBank accession number: MN510470.

201 **Paratype.** MBM286352, station FX-Dive 173 ( $17^\circ 28.12'\text{N}$ ,  $153^\circ 10.07'\text{E}$ ), Kocebu Guyot, depth  
202 1,279 m, 7 April 2018.

203 **Diagnosis.** *Chrysogorgia* “group A, Spiculosae” with a long unbranched stem and a sympodial  
204 branching part with 1/3L branching sequence on the top. Branches subdivided dichotomously, up  
205 to fifth order. Polyps with an expanded base and a slender neck. Rods and spindles of the polyp  
206 neck and tentacles long and coarse, with many warts on surface. Scales at polyp body base  
207 elongated and thick, rarely branched. Scales in coenenchyme flat and elongated with irregular  
208 edges.

209 **Description.** Specimen of holotype about 55 cm in height excluding the holdfast. Colony tree-  
210 shaped, composed of a sympodial branching part on the top and a fragile, slender and  
211 unbranched stem about 35.5 cm long and 1.5 mm in diameter at base (Fig. 4C). Stem surface  
212 almost smooth with a few scars and aeruginous metallic luster, and sometimes covered with a  
213 layer of pink mucous membrane. Branching part produced a slightly zigzag pattern at the top  
214 portion with branching sequence 1/3L. Branches subdivided dichotomously, nearly  
215 perpendicular to the axis, up to fifth order, most broken after collection. Distance between  
216 adjacent branches and the first branch internodes both 15–22 mm long, orthostiche interval 50–  
217 65 mm, and the terminal branches up to 75 mm. Polyps with a long neck and an expanded body  
218 base, 2–4 mm long, 1–2 mm wide at base, with the neck up to 2 mm long and less than 1 mm  
219 wide (Figs. 4E – 4I). Up to two polyps on the first internodes, two to four in middle internodes,  
220 up to ten in terminal branchlets. No polyp on main axis internodes. Golden eggs present in  
221 expanded body bases. Polyps pink immediately after collection, color gradually faded in alcohol.

222       Rods longitudinally arranged in the back of the tentacles, rarely branched, with many small  
223 warts on surface, measuring  $105\text{--}442 \times 14\text{--}50 \mu\text{m}$  (Figs. 4G, 4I, 5A–5G). Rare sclerites extend  
224 into the pinnules, and pinnules free of sclerites. Spindles and rods longitudinally arranged in the  
225 polyp neck, slender with many small warts on surface, sometimes with one or two sharp ends,  
226 measuring  $170\text{--}600 \times 17\text{--}62 \mu\text{m}$  (Figs. 4H, 5H–5L). Scales longitudinally and transversally  
227 arranged at base of expanded polyp body, elongated with a few warts and irregular edges,  
228 sometimes branched, thicker and wider than those in coenenchyme, measuring  $144\text{--}551 \times 34\text{--}$   
229  $106 \mu\text{m}$  (Figs. 4H, 5M–5V). Scales of coenenchyme flat and elongate, rarely with distinctly  
230 irregular edges, measuring  $122\text{--}435 \times 28\text{--}83 \mu\text{m}$  (Figs. 5W–5EE).

231 **Variation of Paratype.** Specimen 65 cm in height with unbranched stem about 35 cm long and  
232 1 mm across at base (Fig. 4D). Branching part relatively longer and more zigzagging.

233 **Type locality.** Kocebu Guyot in the Magellan Seamount chain with water depths of 1,279–1,321  
234 m.

235 **Etymology.** The Latin adjective *fragilis* (fragile) refers to the fragile stem and branches of the  
236 species.

237 **Distribution and habitat.** Found only on the Kocebu Guyot in the Magellan Seamount chain.  
238 Colonies attached to rocky substrate. The holotype was attached with an egg-shaped structure  
239 and the paratype with an individual of the crustacean genus *Galathea* Fabricius, 1793 (Figs. 4A,  
240 4B). The water temperature was about 3.2°C and the salinity about 35.8.

241 **Remarks.** *Chrysogorgia fragilis* sp. nov. belongs to the “group A, Spiculosae” with an unusual  
242 branching sequence of 1/3L, with which it is similar to *Chrysogorgia midas* Cairns, 2018 and *C.*

243 *dendritica* sp. nov. However, the new species differs distinctly from *C. midas* Cairns, 2018 by  
244 the tree-shaped colony (vs. bottlebrush-shaped), wider orthostiche interval (50–65 mm vs. 12–18  
245 mm), larger polyps (2.0–4.0 mm vs. 1.1 mm), and the presence of various shapes of scales at the  
246 body bases (vs. absence). *Chrysogorgia fragilis* sp. nov. is also similar to *C. abludo* Pante &  
247 Watling, 2012 and *C. averta* Pante & Watling, 2012, two species found in the north-western  
248 Atlantic Ocean, in possessing the wide orthostiche interval and long and straight unbranched  
249 stem. However, the new species is easily separated from *C. averta* by the tree-shaped colony (vs.  
250 bottlebrush-shaped). It differs from *C. abludo* by the regular 1/3L branching sequence (vs.  
251 irregular) and elongate flat scales in coenenchyme (vs. small rugged scales) (Table 1).  
252 *Chrysogorgia fragilis* sp. nov. differs from *C. dendritica* sp. nov. by a sympodial branching part  
253 (vs. monopodial) and relatively regular scales at the body bases (vs. amoeba-shaped).

254

255 ***Chrysogorgia gracilis* sp. nov.** (Figs. 6 and 7; Table 1)

256 urn:lsid:zoobank.org:act:F557CE43-D43C-4E5F-86C1-3EFE330A9443

257

258 **Holotype:** MBM286350, station FX-Dive 57 (11°18.34'N, 139°21.43'E), an unnamed seamount  
259 (temporarily named as M2) adjacent to the Mariana Trench, depth 298 m, 23 March 2016.  
260 GenBank accession number: MN510472.

261 **Diagnosis:** *Chrysogorgia* “group A, Spiculosae” with a long unbranched stem and a sympodial  
262 branching part emanating in a regular 1/4L spiral on the top. Stem and branches slender, with  
263 branches subdivided dichotomously. Terminal branchlets gracile and somewhat whip-like.  
264 Polyps small and thin, no more than 1.5 mm long, located on one side of branches. Rods and rod-  
265 like scales slender and abundant in tentacles and at the bases of tentacles. No sclerites at polyp  
266 body base. Scales elongated, rare to absent in coenenchyme. Mesozooids dense along the  
267 internodes of top stem and the bases of branches.

268 **Description.** Specimen orange to reddish after collection, became yellow in alcohol, about 51.8  
269 cm long (Figs. 6B, 6C). Stem and branches golden with slightly glaucous metallic luster. Colony  
270 tree-shaped. Unbranched stem curved, up to 40.5 cm in arc length and 1.0–2.9 mm in diameter,  
271 emanating in regular 1/4L spiral on the top of a tall (Fig. 6C). Holdfast small and rounded, about  
272 9.8–12.5 mm in diameter. Distance between adjacent branches in stem 2.0–4.5 mm long and  
273 orthostiche interval 11–16 mm. The first branch internodes 3–7 mm. Branches subdivided 2–7  
274 times and the angle between bifurcating branches particularly obtuse: 18°–62°. Terminal  
275 branchlets slender, usually whip-like, up to 90 mm long.

276 Polyps translucent, 0.9–1.5 mm long, 0.2–0.4 mm wide, uniserial spaced 2–5 mm on the  
277 branches by one side, with angle random to the branches. Polyp body base golden, without  
278 sclerites (Fig. 6D). Tentacles up to 1.0 mm in length, became white in alcohol. Three to 20  
279 polyps on terminal branchlets and up to ten polyps in branch internodes. Axial internodal polyps  
280 not observed in the stem, where dense mesozooids occurred along the internodes of the stem and  
281 branch bases. Mesozooids bud-like shaped, orange in situ and yellowish in alcohol, without  
282 sclerites, about 0.3–0.5 mm wide and up to 0.4 mm high (Figs. 6A, 6G–6I).

283 Rods and rod-like scales slender, sometimes one end flat and the other end cylindrical, mostly  
284 aggregated in the joints between the tentacles and bodies, or longitudinally along the back of the  
285 tentacles, with dentate projections at one or both ends and coarse, granular warts on surface,  
286 measuring 90–450×15–20 μm (Figs. 6E, 6F, 7A–N). Coenenchyme in branches with a thin  
287 pellucid and calcareous layer in outside of the central axis, sometimes with regular scales  
288 oriented along branches or without scales on branches. Scales elongated with smooth surface and  
289 edges, occasionally with finely serrated edges, usually becoming narrow in middle, rare to absent  
290 in coenenchyme, measuring 50–250×12–38 μm (Figs. 7O–W). All sclerites colorless.

291 **Type locality.** An unnamed seamount (temporarily named as M2) adjacent to the Mariana  
292 Trench with water depths of 298 m.

293 **Etymology.** The Latin adjective *gracilis* (gracile) refers to the gracile stem and branches of this  
294 species.

295 **Distribution and Habitat.** Found only on the M2 seamount adjacent to the Mariana Trench.  
296 Colony attached to a rocky substrate with a small holdfast (Fig. 6A).

297 **Remarks.** Among the species possessing 1/4L branching sequence and rods in tentacles, *C.*  
298 *gracilis* sp. nov. mostly resembles *C. pyramidalis* Kükenthal, 1908 in the same branching  
299 division and similar length, soft and translucent polyp's body, and the very rare sclerites in  
300 coenenchyme (Kükenthal, 1908; Kinoshita, 1913; Cairns, 2001). However, *C. gracilis* sp. nov.  
301 differs from *C. pyramidalis* by its distinctly longer and unbranched stem, more slender rods with  
302 lobed or irregular round ends, nearly smooth and elongated scales in coenenchyme, and the  
303 presence of mesozooids (Kükenthal, 1908; Kinoshita, 1913). Compared with congeners,  
304 *Chrysogorgia gracilis* sp. nov. possesses much thinner and smaller polyps, where no sclerites  
305 occur at the bases, and rare to absent sclerites in coenenchyme. In contrast, both the polyp body  
306 wall and coenenchyme are usually composed of numerous sclerites in other species of  
307 *Chrysogorgia*.

308 The specimen collected is characteristic in having numerous yellowish mesozooids on the  
309 stem internodes and the bases of branches (Figs. 6G–6I). The mesozooids in this species are  
310 distinguished from the nematozooids or cnidae existed in some species of *Chrysogorgia* and  
311 *Iridogorgia* Verrill, 1883 (Kinoshita, 1913; Deichmann, 1936) in size, shape and distribution.  
312 The nematozooids are a kind of small protuberances or verrucae distributed on the surface of  
313 polyps and coenenchyme on branches, while the mesozooids are similar to polyps in width and  
314 are independent on the surface of branches (Fig. 6A).

315

### 316 **Genetic distance and phylogenetic analyses**

317

318 The mtMutS sequences of the three new species were obtained and deposited in GenBank, with  
319 the accession number and the length are as follows: MN510469, 620 bp for *Chrysogorgia*  
320 *dendritica* sp. nov.; MN510470, 635 bp for *C. fragilis* sp. nov.; and MN510472, 635 bp for *C.*  
321 *gracilis* sp. nov. The alignment dataset comprised 623 nucleotide positions. The present  
322 intraspecific distances were calculated based on *C. abludo*, *C. tricaulis*, *C. artospira*, *C. averta*

323 and *C. chryseis* populations, and no intraspecific variability was observed for the four species  
324 (Table 2). The mtMutS genetic distances among the species of *Chrysogorgia* range from zero to  
325 2.42% (Table 2). The genetic distances between the new species *C. fragilis* sp. nov. and  
326 congeners are in the range of 0.16%–2.26%, and those between *C. gracilis* sp. nov. and  
327 congeners are in the range of 0.48%–2.10% (Table 2). No genetic variability was observed  
328 between *dendritica* sp. nov. and *C. abludo*, and the genetic distances between this new species  
329 and the rest congeners range from 0.16% to 2.42% (Table 2).

330 The ML and BI phylogenetic trees are identical in topology, and thus only the former with  
331 the both support values was showed (Fig. 8). The *Chrysogorgia* species were separated into two  
332 main clades (Clade I and II) with high support values. Clade I includes *C. binata*, *C. cf. stellata*  
333 and *C. chryseis*, and Clade II contains all the rest species. The new species *C. dendritica* sp. nov.  
334 and *C. abludo* formed a sister subclade, followed by *C. fragilis* sp. nov. *Chrysogorgia gracilis*  
335 sp. nov. formed a sister subclade with *C. tricaulis*, *C. artospira*, *C. pinnata*, *C. averta* and the  
336 subclade *C. ramificans* + *C. monticola*.

337

## 338 Discussion

339

340 Both the morphology and molecular phylogenetic analysis supported the assignment of the three  
341 new species to the genus *Chrysogorgia*. The genetic distance analysis of mtMutS is considered  
342 as one of the first steps in an integrative identification of octocorals ([McFadden et al., 2011](#);  
343 [Pante et al., 2012](#)). In the present study, however, the mtMutS genetic distances within  
344 *Chrysogorgia* are relatively low, and there is no barcoding gap (intraspecific zero vs.  
345 interspecific 0–2.42%) for species separation. Alternatively, single mutations on mtMutS,  
346 corresponding to the genetic distance of ca. 0.16%, can be used to separate *Chrysogorgia* species  
347 ([Pante & Watling, 2012](#); [Pante et al., 2015](#); [this study](#)). *Chrysogorgia gracilis* sp. nov. and *C.*  
348 *fragilis* sp. nov. showed at least one single mutation difference from congeners (the  
349 corresponding genetic distances in range of 0.16%–2.26%; Table 2), supporting the  
350 establishment of the two new species. Although no genetic variability was observed between *C.*  
351 *dendritica* sp. nov. and *C. abludo*, the former is distinctly different from the latter by its unique  
352 monopodial stem and the amoeba-shaped sclerites at the polyp body bases.

353 Based on the diagnosis sensu [Pante & Watling, 2012](#) and [Cordeiro et al., 2015](#), the genus  
354 *Chrysogorgia* includes three branching forms: a single ascending spiral (clockwise or  
355 counterclockwise), a fan (planar colony) and two fans emerging from a short main stem  
356 (biflabellate colony). Based on the phylogenetic analysis, all the available *Chrysogorgia* species  
357 could be separated into two groups (Clade I and II). All species in Clade I (*C. binata*, *C. cf.*  
358 *stellata* and *C. chryseis*) have a bi- or multi-flabellate colony, as in the type species *C.*  
359 *desbonni* Duchassaing & Michelotti, 1864. The other species of *Chrysogorgia* possessing either  
360 a bottlebrush-shaped, a planar or a tree-shaped colony formed the Clade II with high support (Fig.  
361 8). Furthermore, the genetic distances between Clade I and II are much higher than the intra-  
362 clade ones of Clade I (1.45%–2.42% vs. 0–0.48%; Table 2). Likely, Clade II represents a new

363 subgroup of *Chrysogorgia* or even a new genus. However, only the sequences from 12 of 75  
364 *Chrysogorgia* species are available for the genetic analysis. Further integrated genetic and  
365 morphological analyses are needed to verify this suggestion.

366 It is worth of note that all the new species possess a tree-shaped colony (monopodial,  
367 sympodial), which represent a new colony form in *Chrysogorgia*. Such a colony occurs also in  
368 the paratype NAS204-1 of *C. abludo* (Pante & Watling, 2012). Therefore, we add the tree-  
369 shaped colony to the diagnosis of the genus. Here, we extend the diagnosis of *Chrysogorgia* on  
370 the basis of Pante & Watling (2012) and Cordeiro et al. (2015): Colony branching usually  
371 sympodial, occasionally monopodial, arising from a single ascending spiral (clockwise or  
372 counterclockwise, bottlebrush-shaped colony), a fan (planar colony), two fans emerging from a  
373 short main stem (biflabellate colony), or an unbranched main stem forming a tree-shaped colony.  
374 Axis with a metallic shine, dark to golden in color. Branch subdivided dichotomously or  
375 pinnately. Most polyps relatively large to the size of the branches they sit on, few in number and  
376 well separated from one another. Sclerites in the form of spindles, rods, scales and rare plates  
377 with little ornamentation.

378

### 379 **Conclusions**

380

381 Based on the morphological and phylogenetic analyses, the newly sampled specimens are  
382 recognized as three new species *Chrysogorgia dendritica* sp. nov., *C. fragilis* sp. nov. and *C.*  
383 *gracilis* sp. nov. Furthermore, the tree-shaped colony of the new species represents a new  
384 branching pattern of *Chrysogorgia*, and therefore we extend the generic diagnosis.

385

### 386 **Acknowledgements**

387 We thank the assistance of the crew of R/V *KeXue* and ROV *FaXian* for sample collection. We  
388 also thank Dr. Yang Li for comments on an early manuscript and Mr. Shaoqing Wang for taking  
389 the photos on board.

390

### 391 **Additional Information and Declarations**

#### 392 **Competing Interests**

393 The authors declare there are no competing interests.

394

#### 395 **Author Contributions**

396 Yu Xu conceived and designed the experiments, performed the experiments, analyzed the  
397 morphological data, prepared figures and tables, authored drafts of the paper, approved the final  
398 draft.

399 Zifeng Zhan analyzed the molecular data, prepared figures and tables, authored drafts of the  
400 paper, approved the final draft.

401 Kuidong Xu conceived and designed the experiments, reviewed drafts of the paper, approved the  
402 final draft.

403

**404 Data Availability and DNA Deposition**

405 The following information was supplied regarding data availability:

406 The specimens described in this study are deposited in the Marine Biological Museum of  
407 Chinese Academy of Sciences (MBMCAS) at Institute of Oceanology, Qingdao, China. Voucher  
408 ID for *Chrysogorgia dendritica* is MBM286354; vouchers ID for the holotype and paratypes  
409 of *Chrysogorgia fragilis* are MBM286351 and MBM286352, respectively; Voucher ID for  
410 *Chrysogorgia gracilis* is MBM286350. The mtMuts sequences of the new species are available  
411 at NCBI GenBank: MN510469, MN510470 and MN510472, respectively.

412

**413 New Species Registration**

414 The following information was supplied regarding the registration of a newly described species:

415 Publication LSID: urn:lsid:zoobank.org:pub:00D5E053-EFF8-4142-8D16-AAFC17D028E2.

416 *Chrysogorgia dendritica* sp. nov. LSID: urn:lsid:zoobank.org:act:F0050AD3-9E65-4B03-8D26-

417 2C687018DCAD, *Chrysogorgia fragilis* sp. nov. LSID: urn:lsid:zoobank.org:act:562CFDA7-

418 88F5-4D81-8FE5-BDE1F56A3EEC, and *Chrysogorgia gracilis* sp. nov. LSID:

419 urn:lsid:zoobank.org:act:F557CE43-D43C-4E5F-86C1-3EFE330A9443.

420

**421 Funding**

422 This work was supported by the Key Program of National Natural Science Foundation of China  
423 (No. 41930533), the Strategic Priority Research Program of the Chinese Academy of Sciences  
424 (XDA19060401), the Science & Technology Basic Resources Investigation Program of China  
425 (2017FY100804) and the Senior User Project of RV KEXUE.

426

**427 References**

428 **Alfaro ME, Zoller S, Lutzoni F. 2003.** Bayes or Bootstrap? A simulation study comparing the  
429 performance of Bayesian Markov chain Monte Carlo sampling and bootstrapping in  
430 assessing phylogenetic confidence. *Molecular Biology and Evolution* **20**(2): 255–266.

431 **Bayer FM, Grasshoff M, Verseveldt J. 1983.** Illustrated Trilingual Glossary of Morphological  
432 and Anatomical Terms Applied to Octocorallia. E. J. Brill/Dr. W. Backhuys, Leiden, 75 pp.

433 **Cairns SD. 2001.** Studies on western Atlantic Octocorallia (Gorgonacea: Ellisellidae). Part 1:

434 The genus *Chrysogorgia* Duchassaing & Michelotti, 1864. *Proceedings of the Biological*  
435 *Society of Washington* **114**(3): 746–787.

436 [https://doi.org/10.2988/0006-324X\(2007\)120\[243: SOWAOG\] 2.0.CO;2](https://doi.org/10.2988/0006-324X(2007)120[243:SOWAOG]2.0.CO;2)

437 **Cairns SD. 2018.** Deep-Water Octocorals (Cnidaria, Anthozoa) from the Galápagos and Cocos  
438 Islands. Part 1: Suborder Calcaxonia. *ZooKeys* **729**: 1–46.

439 <https://doi.org/10.3897/zookeys.729.21779>

440 **Cordeiro RTS, Castro CB, Pérez CD. 2015.** Deep-water octocorals (Cnidaria: Octocorallia)  
441 from Brazil: family Chrysogorgiidae Verrill, 1883. *Zootaxa* **4058**(1): 81–100.

442 <https://doi.org/10.11646/zootaxa.4058.1.4>

- 443 **Darriba D, Taboada GL, Doallo R, Posada D. 2012.** jModelTest 2: more models, new  
444 heuristics and parallel computing. *Nature Methods* **9**: 772.
- 445 **Deichmann, E. 1936.** The Alcyonaria of the western part of the Atlantic Ocean. *Memoirs of the*  
446 *Museum of Comparative Zoology, Harvard*, **53**, 1–317.
- 447 **Duchassaing P, Michelotti J. 1864.** Supplément au mémoire sur les coralliaires des Antilles.  
448 *Memorie della Reale Accademia delle Scienze di Torino* **2(23)**: 97–206
- 449 **Ehrenberg CG. 1834.** Beiträge zur physiologischen Kenntniss der Corallenthiere im  
450 allgemeinen, und besonders des rothen Meeres, nebst einem Versuche zur physiologischen  
451 Systematik derselben. *Abhandlungen der Königlich Akademie der Wissenschaften, Berlin*  
452 **1**: 225–380.
- 453 **Grasshoff M. 1999.** The shallow-water gorgonians of New Caledonia and adjacent islands  
454 (Coelenterata, Octocorallia). *Senckenbergiana biologica* **78**: 1–121.
- 455 **Guindon S, Dufayard JF, Lefort V, Anisimova M, Hordijk W, Gascuel O. 2010.** New  
456 algorithms and methods to estimate maximum-likelihood phylogenies: assessing the  
457 performance of PhyML 3.0. *Systematic Biology* **59**: 307–321.
- 458 **Haeckel E. 1866.** Generelle morphologie der Organismen, vol. 2. Verlag von Georg Reimer,  
459 Berlin.
- 460 **Hall TA. 1999.** BioEdit: a user-friendly biological sequence alignment editor and analysis  
461 program for Windows 95/98/NT. *Nucleic Acids Symposium Series*, **41**, 95–98.
- 462 **Herrera S, Baco A, Sánchez JA. 2010.** Molecular systematics of the bubblegum coral genera  
463 (Paragorgiidae, Octocorallia) and description of a new deep-sea species. *Molecular*  
464 *Phylogenetics and Evolution* **55(1)**: 123–135.
- 465 **Hillis DM, Bull JJ. 1993.** An empirical test of bootstrapping as a method for assessing  
466 confidence in phylogenetic analysis. *Systematic Biology* **42(2)**: 182–192.
- 467 **Katoh K, Standley DM. 2013.** MAFFT Multiple Sequence Alignment Software version 7:  
468 improvements in performance and usability. *Molecular Biology and Evolution* **30**: 772–780.
- 469 **Kinoshita K. 1913.** Studien über einige Chrysogorgiiden Japans. *Journal of the College of*  
470 *Science, Tokyo Imperial University* **33(2)**: 47 pp.
- 471 **Kükenthal, W. 1908.** Diagnosen neuer Gorgoniden aus der Gattung *Chrysogorgia* (6.  
472 Mitteilung). *Zoologischer Anzeiger* **33(21)**: 704–708.
- 473 **Lamouroux JVF. 1812.** Extrait d'un mémoire sur la classification des polypiers coralligènes non  
474 entièrement pierreux. *Nouveau Bulletin des Sciences, Société Philomathique de Paris* **3(63)**:  
475 181–188.
- 476 **McFadden CS, Benayahu Y, Pante E, Thoma JN, Nevarez PA, France SC. 2011.** Limitations  
477 of mitochondrial gene barcoding in Octocorallia. *Molecular Ecology Resources* **11(1)**:19–  
478 31.
- 479 **Pante E, France SC. 2010.** *Pseudochrysogorgia bellona* n. gen., sp. nov.: a new genus and  
480 species of chrysogorgiid octocoral (Coelenterata, Anthozoa) from the Coral Sea.  
481 *Zoosystema* **32(4)**: 595–612.  
482 <https://doi.org/10.5252/z2010n4a4>

- 483 **Pante E, Watling L. 2012.** *Chrysogorgia* from the New England and Corner Seamounts:  
484 Atlantic–Pacific connections. *Journal of the Marine Biological Association of the United*  
485 *Kingdom* **92**(5): 911–927.  
486 <http://doi.org/10.1017/S0025315411001354>
- 487 **Pante E, Abdelkrim J, Viricel A, Gey D, France SC, Boisselier MC, Samadi S. 2015.** Use of  
488 rad sequencing for delimiting species. *Heredity* **114**: 450–459.
- 489 **Pante E, France SC, Couloux A, Cruaud C, McFadden CS, Samadi S, Watling L. 2012.**  
490 Deep-sea origin and in-situ diversification of chrysogorgiid octocorals. *PLoS ONE* **7**(6):  
491 e38357.
- 492 **Ronquist FR, Huelsenbeck JP. 2003.** MrBayes 3: Bayesian phylogenetic inference under mixed  
493 models. *Bioinformatics* **19**: 1572–1574.
- 494 **Sánchez JA, Lasker HR, Taylor DJ. 2003.** Phylogenetic analyses among octocorals (Cnidaria):  
495 mitochondrial and nuclear DNA sequences (lsu-rRNA, 16S and ssu-rRNA, 18S) support  
496 two convergent clades of branching gorgonians. *Molecular Biology and Evolution* **29**: 31–  
497 42.
- 498 **Tamura K, Stecher G, Peterson D, Filipowski A, Kumar S. 2013.** MEGA6: Molecular  
499 Evolutionary Genetics Analysis Version 6.0. *Molecular Biology and Evolution* **30**(12):  
500 2725–2729.
- 501 **Verrill AE. 1883.** Report on the Anthozoa, and on some additional species dredged by the  
502 "Blake" in 1877–1879, and by the U.S. Fish Commission steamer "Fish 126 Hawk" in  
503 1880–82. *Bulletin of the Museum of Comparative Zoology* **11**: 1–72.
- 504 **Versluys J. 1902.** Die Gorgoniden der Siboga-Expedition. 1. Die Chrysogorgiiden. *Siboga*  
505 *Expeditie* **13**: 1–120.
- 506 **Watling L, France S, Pante E, Simpson A. 2011.** Biology of Deep-Water Octocorals. In:  
507 Lesser, M. (Ed), *Advances in Marine Biology*. Elsevier Academic press, London, pp. 41–  
508 122.
- 509 **Yang Li, Zifeng Zhan, Kuidong Xu. 2017.** Morphology and molecular phylogeny of  
510 *Paragorgia rubra* sp. nov. (Cnidaria: Octocorallia), a new bubblegum coral species from a  
511 seamount in the tropical Western Pacific. *Chinese Journal of Oceanology and Limnology*  
512 **35**(4): 803–814.  
513 <http://dx.doi.org/10.1007/s00343-017-5320-5>
- 514 **Yu Xu, Yang Li, Zifeng Zhan, Kuidong Xu. 2019.** Morphology and phylogenetic analysis of  
515 two new deep-sea species of *Chrysogorgia* (Cnidaria, Octocorallia, Chrysogorgiidae) from  
516 Kocebu Guyot (Magellan seamounts) in the Pacific Ocean. *Zookeys* **881**: 91–107.  
517 <https://doi.org/10.3897/zookeys.881.34759>

**Table 1** (on next page)

Morphological comparisons between *C. averta* , *C. abludo* , *C. dendritica* sp. nov., *C. fragilis* sp. nov. and *C. gracilis* sp. nov.

1 **Table 1 Morphological comparisons between *C. averta*, *C. abludo*, *C. dendritica* sp. nov., *C.*  
 2 *fragilis* sp. nov. and *C. gracilis* sp. nov.**

Characters/species	<i>C. averta</i>	<i>C. abludo</i>	<i>C. fragilis</i> sp. nov.	<i>C. dendritica</i> sp. nov.	<i>C. gracilis</i> sp. nov.
Group type	A	A	A	A	A
Colony shape	bottlebrush-shaped	bottlebrush-shaped or tree-shaped	tree-shaped	tree-shaped	tree-shaped
Branching sequence	3/8L	1/3, 1/4L, irregular	1/3L	1/3L	1/4L
Interbranch distance (mm)	9–13	4.3–15.0	15–22	16–22	2.0–4.5
Orthostiche interval (mm)	75–78	No data	50–65	50–55	11–16
First branch internode (mm)	13–19	6.1–16.0	15–22	15–20	3–7
Polyps on internodes	0–2	1–2	0–4	1–5	1–10
Polyps on terminal branchlets	1–3	1–6	1–10	1–6	3–20
Polyps height (mm)	1.1–1.9	0.8–2.2	2.0–4.0	3.0	0.9–1.5
Sclerites in coenenchyme	rods and scales	small rugged scales	elongate flat scales	flat and lobed scales	elongated scales with smooth surface and edges
Sclerites in body wall	scales and rods	scales and rods	scales, rods and spindles	plates, scales, rods and spindles	scales and rods
Sclerites in tentacles	rods	rods	rods	rods	scales and rods
Distribution	North Atlantic	North Atlantic	Western Pacific	Western Pacific	Western Pacific
References	Pante & Watling 2012	Pante & Watling 2012	Present study	Present study	Present study

3

4

**Table 2** (on next page)

Interspecific and intraspecific uncorrected pairwise distances at mtMutS of species of *Chrysogorgia*.

1 **Table 2 Interspecific and intraspecific uncorrected pairwise distances at mtMutS of species of *Chrysogorgia*.**

2

	1	2	3	4	5	6	7	8	9	10	11	12	13	
<i>Chrysogorgia gracilis</i> sp. nov.														
1	<b>MN510472</b>	-												
2	<b><i>C. dendritica</i> sp. nov. MN510469</b>	0.97%	-											
3	<b><i>C. fragilis</i> sp. nov. MN510470</b>	1.13%	0.16%	-										
4	<i>C. abludo</i> GQ180139, JN227999	0.97%	0	0.16%	0									
	<i>C. tricaulis</i> JN227998, JN227990,													
5	JN227991, GQ180123-31, EU268056	0.65%	0.97%	0.81%	0.97%	0								
6	<i>C. artospira</i> GQ180132-5, GQ353317	0.48%	0.81%	0.65%	0.81%	0.16%	0							
7	<i>C. pinnata</i> JN227988	0.48%	0.81%	0.65%	0.81%	0.16%	0	-						
8	<i>C. averta</i> KC788265, GQ180136	0.81%	1.13%	0.97%	1.13%	0.48%	0.32%	0.32%	0					
9	<i>C. ramificans</i> MK431863	1.13%	1.45%	1.29%	1.45%	0.81%	0.65%	0.65%	0.97%	-				
10	<i>C. monticola</i> JN227989	1.13%	1.45%	1.29%	1.45%	0.81%	0.65%	0.65%	0.97%	0.32%	-			
11	<i>C. binata</i> MK431862	2.10%	2.42%	2.26%	2.42%	1.77%	1.61%	1.61%	1.94%	2.26%	2.26%	-		
12	<i>C. cf. stellata</i> JN227920	1.94%	2.26%	2.10%	2.26%	1.61%	1.45%	1.45%	1.77%	2.10%	2.10%	0.16%	-	
13	<i>C. chryseis</i> JN227992, DQ297421	2.10%	2.42%	2.26%	2.42%	1.77%	1.61%	1.61%	1.94%	2.26%	2.26%	0.48%	0.32%	0

3

## Figure 1

Sampling sites on a seamount (M2) adjacent to the Mariana Trench and the Kocebu Guyot in the Western Pacific Ocean.

(Map credit: ODV at <http://odv.awi.de/>, plotted by Yu Xu).

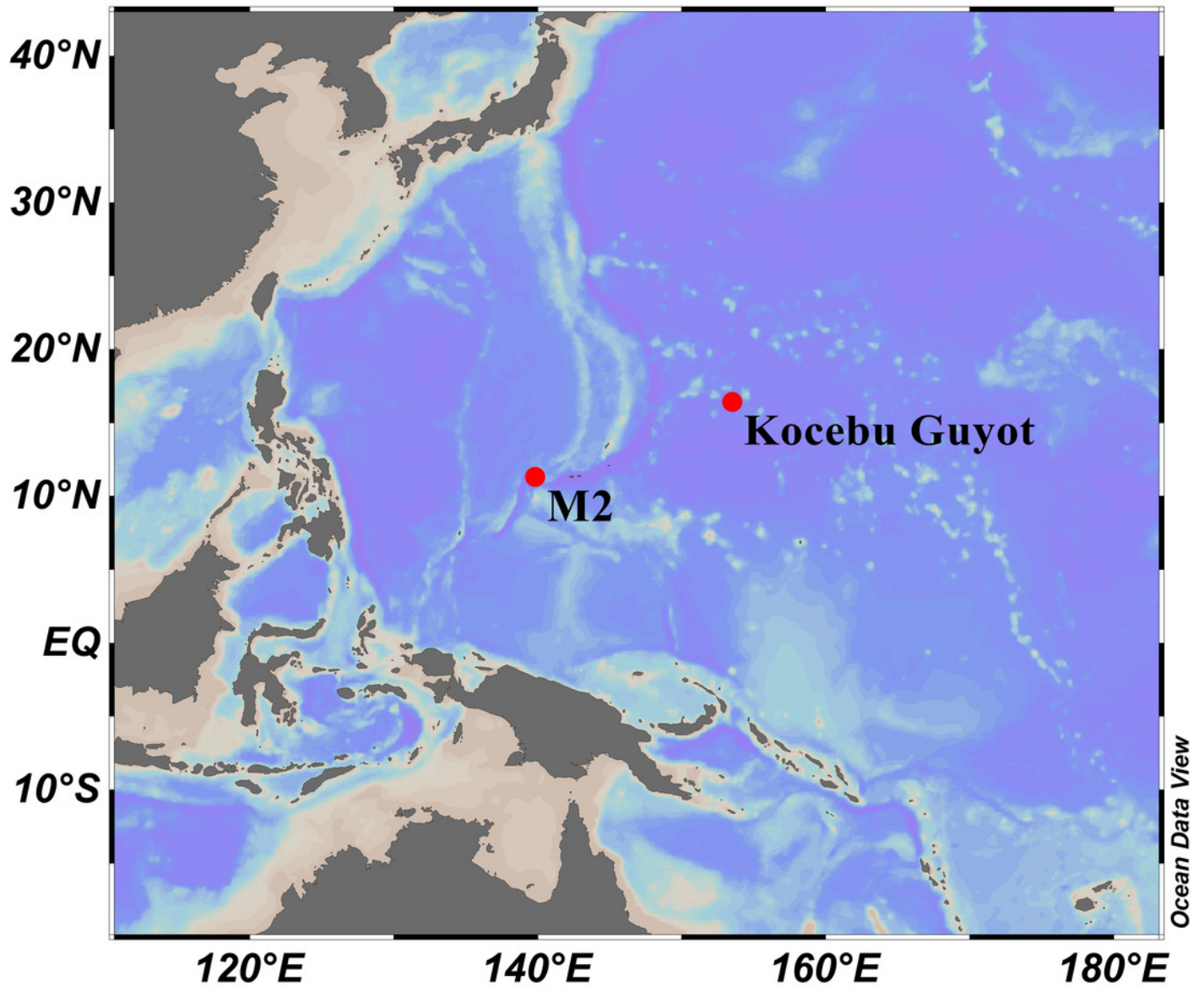


## Figure 2

The external morphology and polyps of *Chrysogorgia dendritica* sp. nov..

**(A) The holotype in situ; (B) The holotype immediately after collection; (C) A single polyp under light microscope; (D) Single polyp under SEM. (E) Tentacles with rods under SEM (Photo credit: Yu Xu and Shaoqing Wang).**

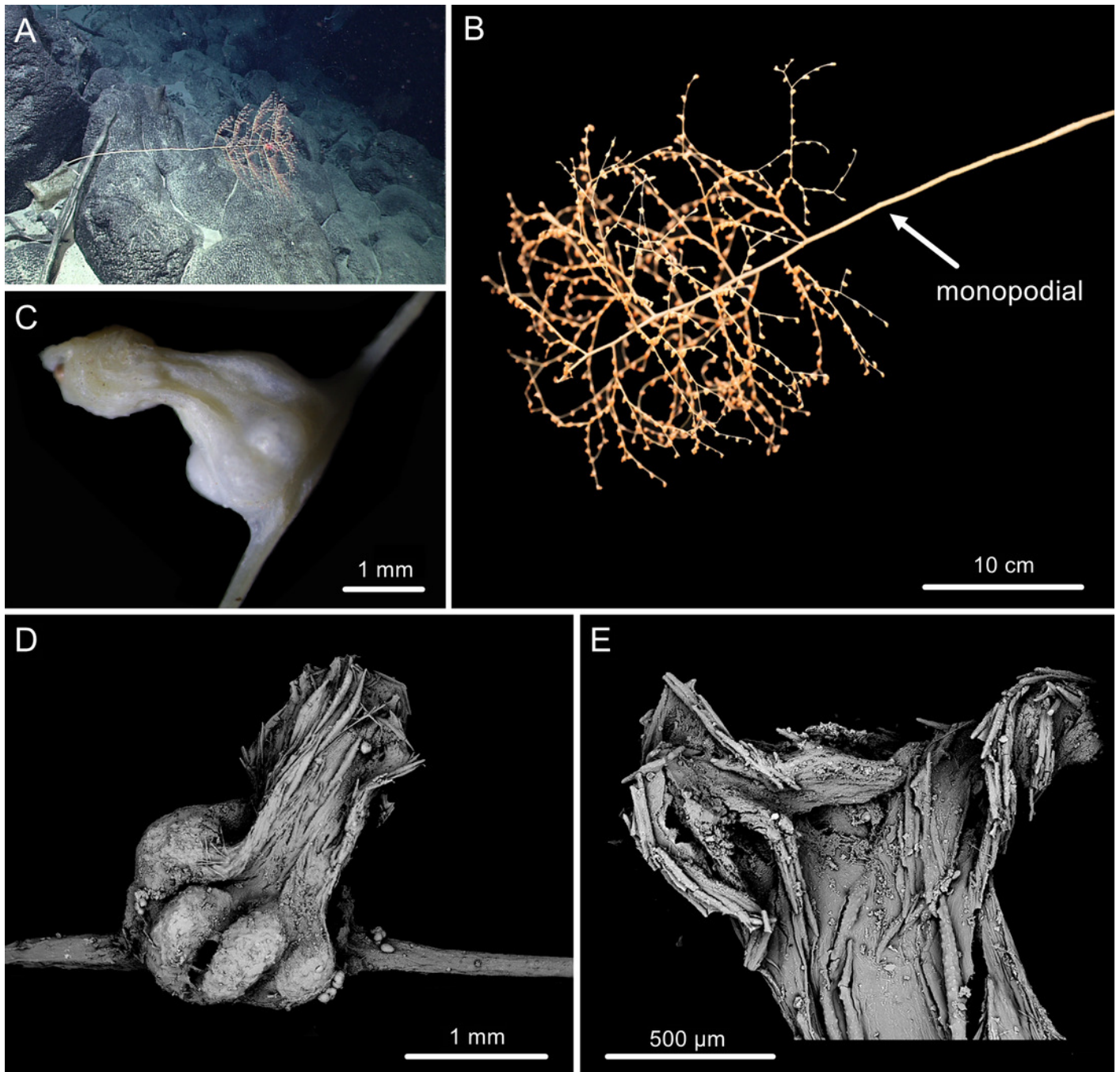


## Figure 3

Sclerites of *Chrysogorgia dendritica* sp. nov. .

**(A-G) Sclerites of the polyp neck. (H-M) Sclerites in the back of tentacles; (N-X) Sclerites at the body base; (Y-GG) Sclerites in coenenchyme. Scale bars: A-G and H-M, N-X and Y-GG at the same scale, respectively (Image credit: Yu Xu).**

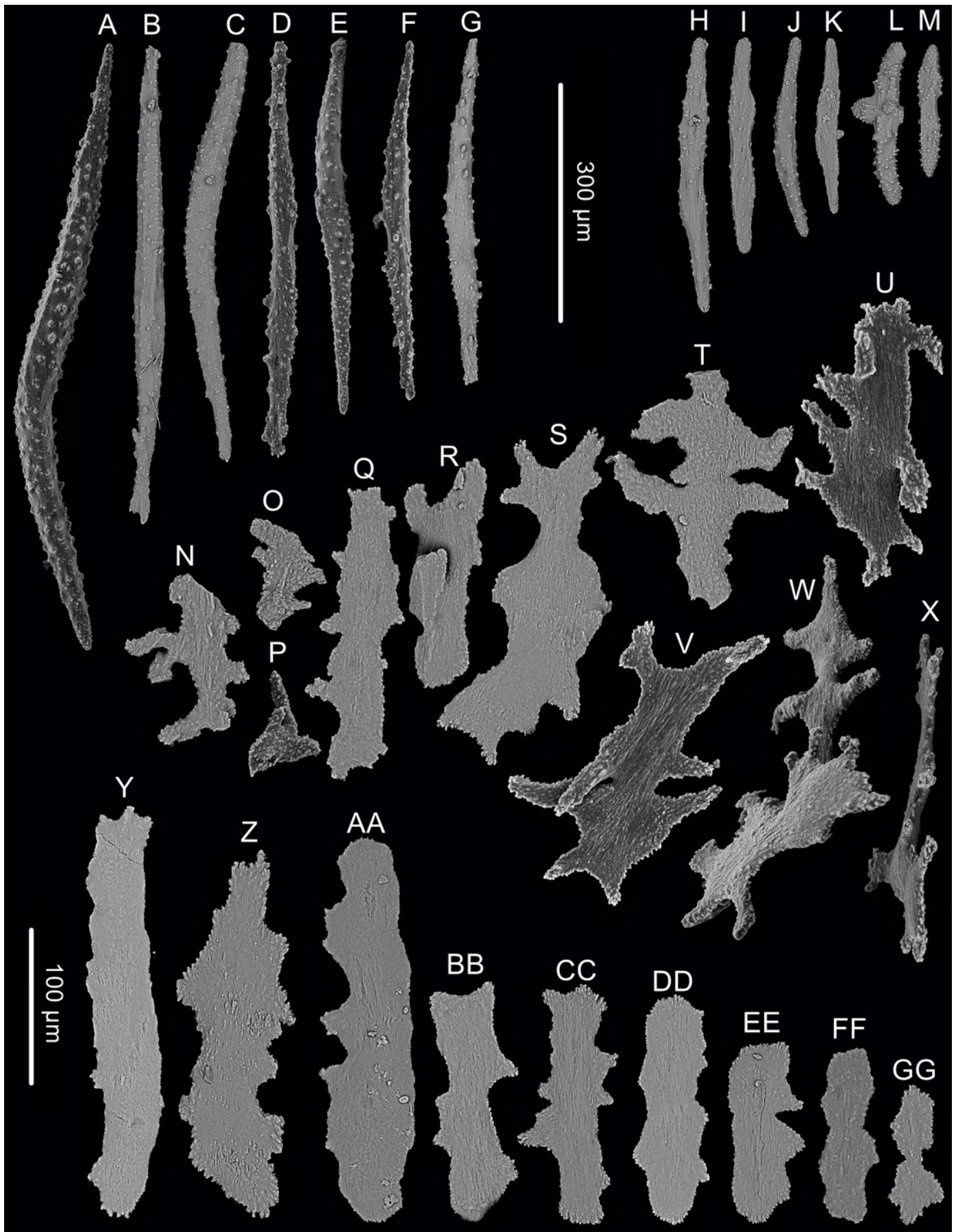


## Figure 4

The external morphology and polyps of *Chrysogorgia fragilis* sp.nov..

**(A) The holotype in situ. Laser dots spaced at 33 cm used for measuring dimensions; (B) The paratype in situ; (C) The holotype immediately after collection; (D) The paratype after fixation; (E, F) A single polyp under light microscope; (G-I) Three polyps under SEM (Photo credit: Yu Xu and Shaoqing Wang).**

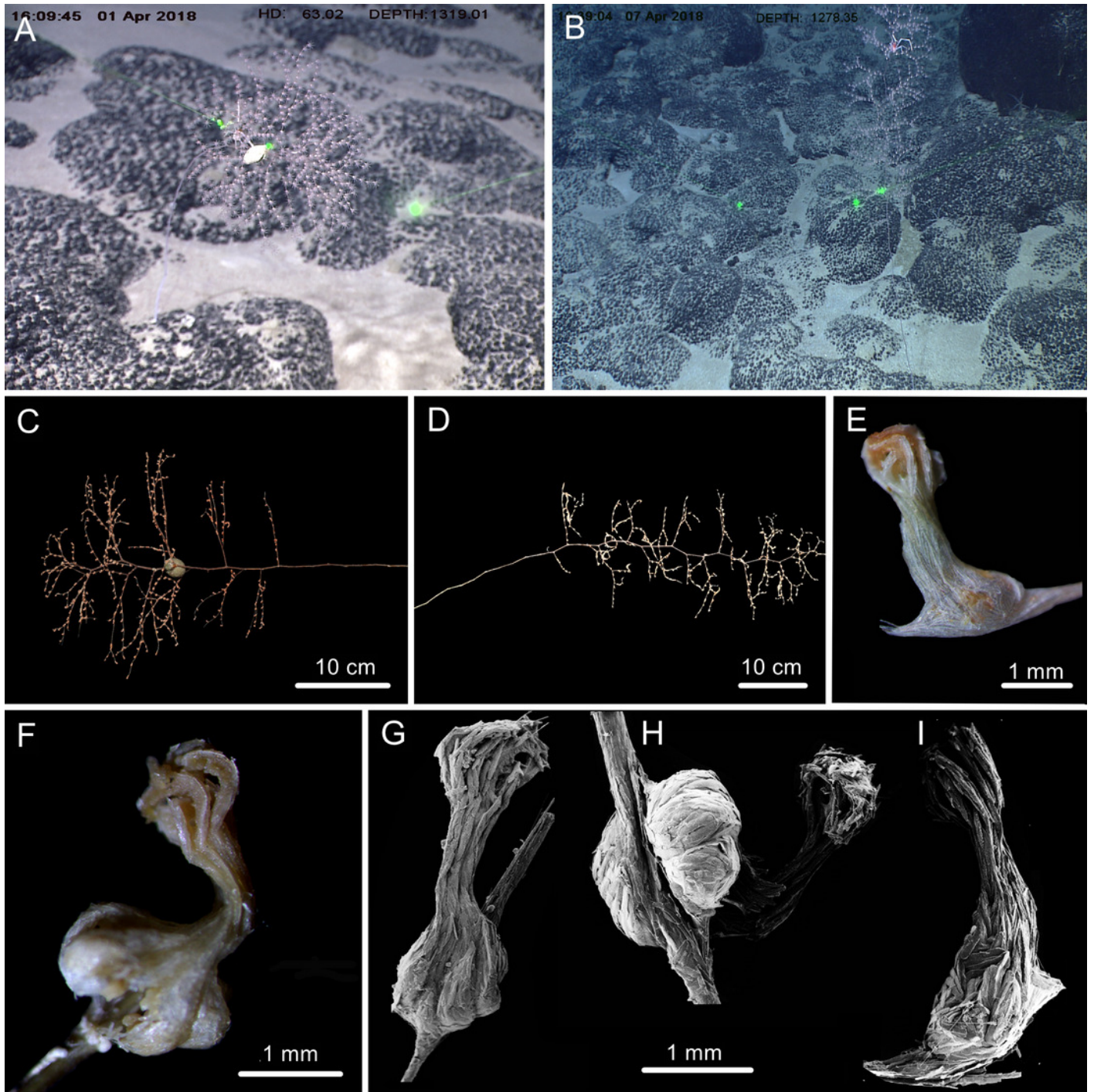


## Figure 5

Sclerites of *Chrysogorgia fragilis* sp.nov..

**(A-G) Sclerites of the polyp neck; (H-L) Sclerites in the back of tentacles; (M-V) Sclerites at the expanded polyp body base; (W-EE) Sclerites in coenenchyme. Scale bar: all at the same scale (Image credit: Yu Xu).**

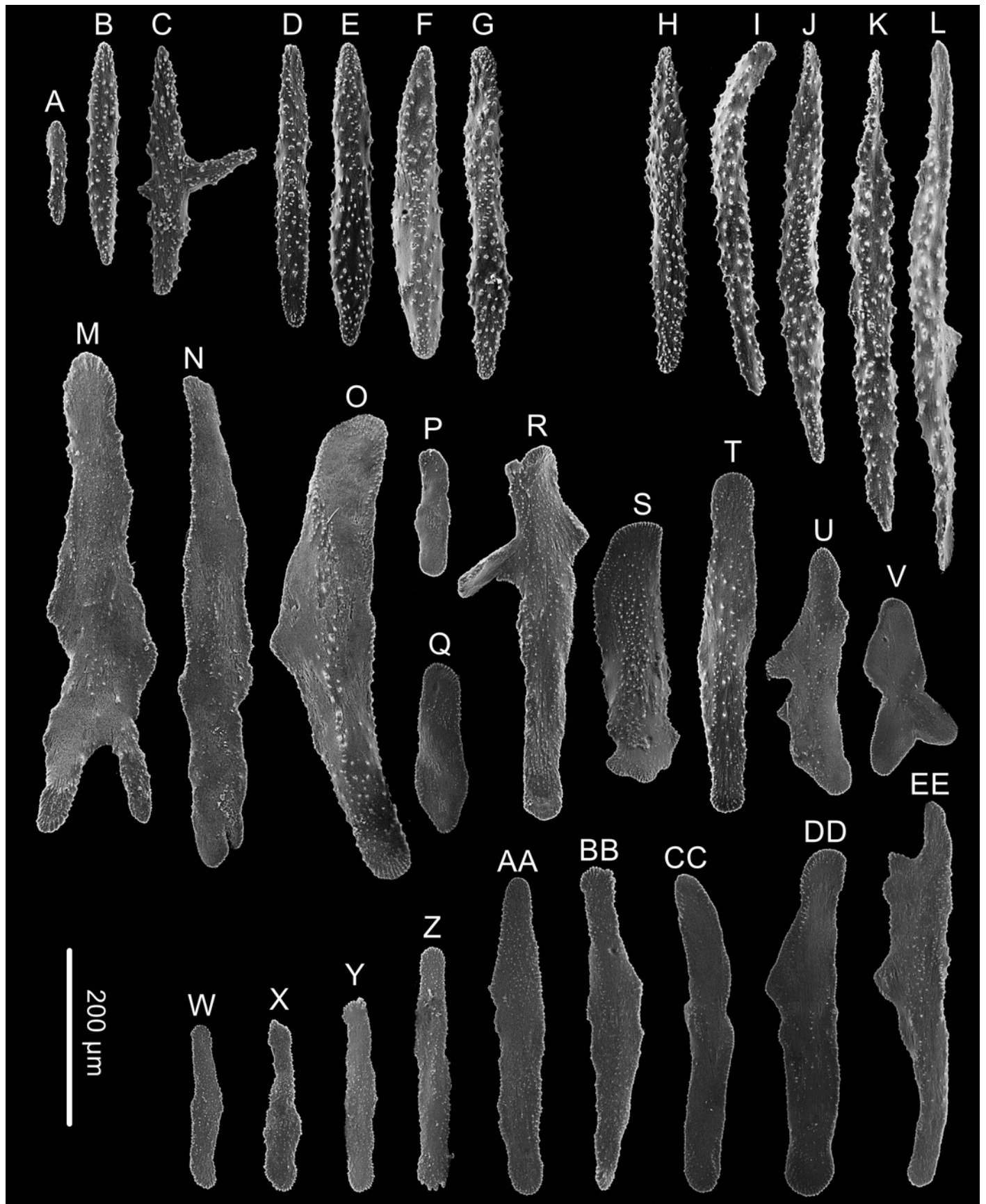


## Figure 6

The external morphology and polyps of the holotype of *Chrysogorgia gracilis* sp. nov..

**(A-C) The holotype in situ (A) and after collection (B) and fixation (C); Laser dots spaced at 33 cm used for measuring dimensions; (D) A single polyp under light microscope; (E) A single polyp under SEM; (F) Tentacles under SEM; (G) Mesozooids at the base of branch under light microscope; (H) Four mesozooids under SEM; (I) A single mesozooid under SEM (Photo credit: Yu Xu and Shaoqing Wang).**

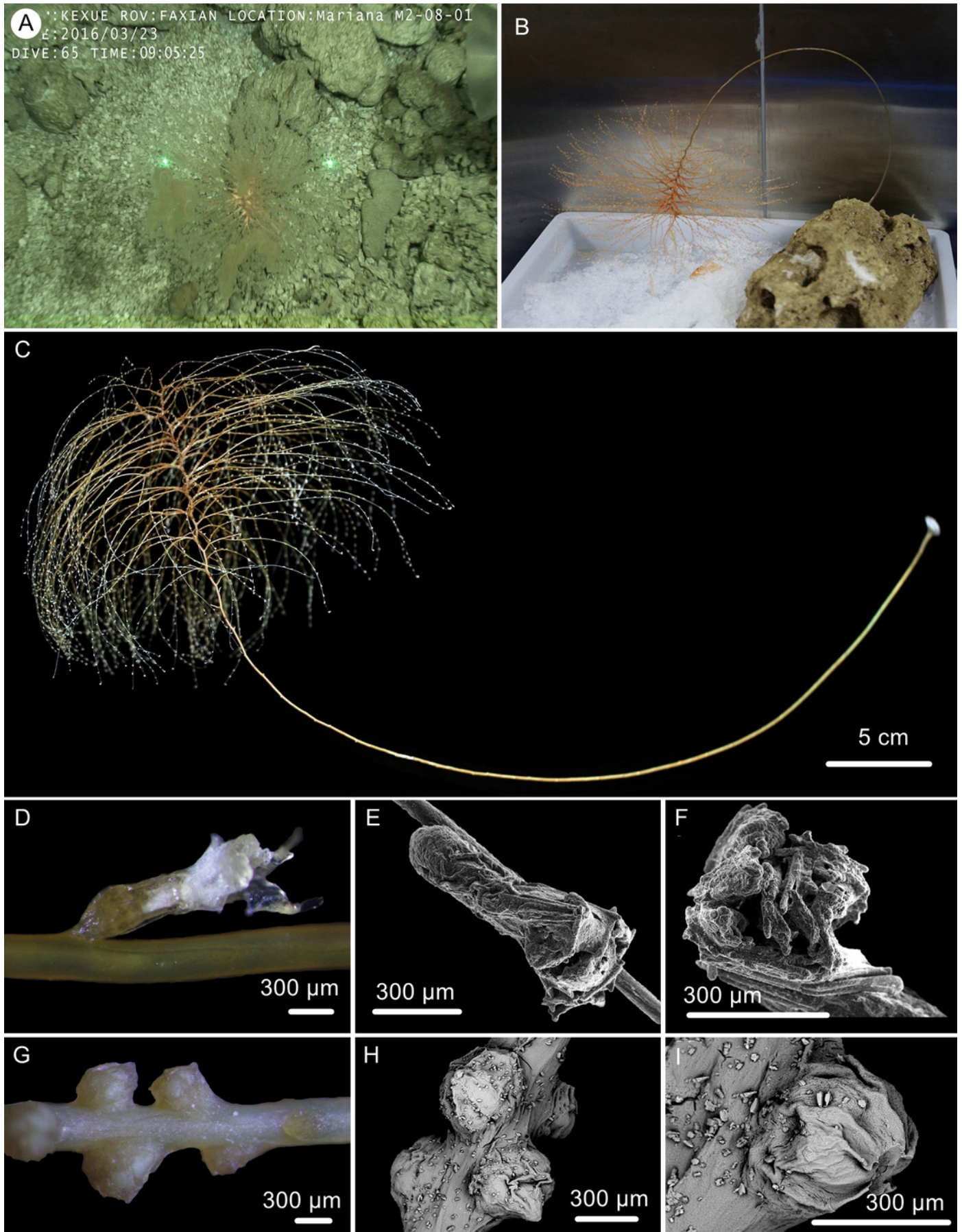


## Figure 7

Sclerites of *Chrysogorgia gracilis* sp. nov..

**(A-N) Sclerites in tentacles and at the bases of tentacles; (O-W) Sclerites in coenenchyme.**  
**Scales bars: all at the same scale (Image credit: Yu Xu).**

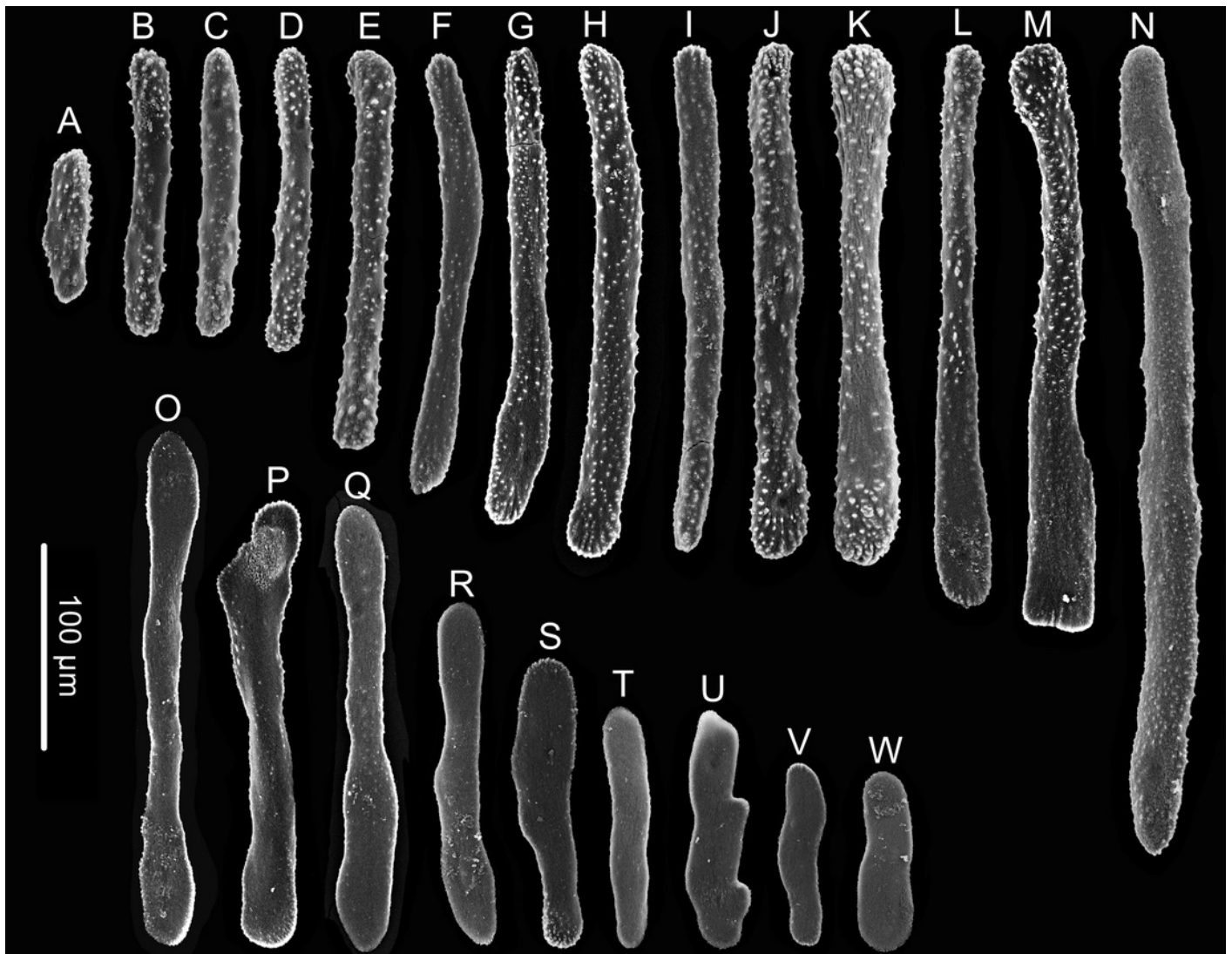


## Figure 8

Maximum likelihood (ML) tree inferred from the mtMutS sequences of *Chrysogorgia* and the related species sequences.

**The Bayesian inference (BI) tree and the ML tree are identical in topology. Node support is as follows: BI posterior probability / ML bootstrap. Newly sequenced species are in bold (Image credit: Zifeng Zhan).**

